ISSN 1063-7834, Physics of the Solid State, 2020, Vol. 62, No. 7, pp. 1165–1171. © Pleiades Publishing, Ltd., 2020.
Russian Text © The Author(s), 2020, published in Fizika Tverdogo Tela, 2020, Vol. 62, No. 7, pp. 1036–1042.

MAGNETISM

Single-Ion Weak Antiferromagnetism and Spin-Flop Transition in a Two-Sublattice Ferromagnet

S. N. Martynov*

Kirensky Institute of Physics, Krasnoyarsk Scientific Center, Siberian Branch, Russian Academy of Sciences, Krasnoyarsk, 660036 Russia

**e-mail: unonav@iph.krasn.ru*

Received January 31, 2020; revised January 31, 2020; accepted February 4, 2020

Abstract—The ground state of a Heisenberg ferromagnet with the noncollinear single-ion anisotropy axes of two magnetic sublattices has been investigated in an external magnetic field applied in the anisotropy axes plane. Noncollinearity of the sublattice local anisotropy axes leads to a new effect called the orientational first-order spin-flop phase transition. The transition field depends on the single-ion anisotropy value and sublattice local axes orientation. An analysis of the stability of magnetic states shows that the transition is accompanied by the hysteretic field dependence of the magnetization. The dependences of the spin-flop transition field, magnetization jump, and susceptibility on the single-ion anisotropy value and axes orientation have been determined. The results obtained are used to explain the field dependence of the magnetization in the $PbMnBO_4$ ferromagnetic crystal.

Keywords: ferromagnetism, single-ion anisotropy, orientational phase transition

DOI: 10.1134/S1063783420070148

1. INTRODUCTION

The term "weak antiferromagnetism" was introduced by Vonsovsky and Turov [1–3] by analogy with the weak ferromagnetism to define the magnetic ordering in a magnet with the basic ferromagnetic exchange and sublattice noncollinearity caused by the Dzyaloshinskii–Moriya (DM) relativistic exchange [4, 5]

$$H_{\mathrm{DM}} = \mathbf{D}[\mathbf{M}_1 \times \mathbf{M}_2],$$

where M_1 and M_2 are the magnetic moments of sublattices. At the ordering of this type, the absolute value of the antiferromagnetism vector l is small as compared with the total magnetic moment m

$$|\mathbf{l}| = |\mathbf{M}_1 - \mathbf{M}_2| \ll |\mathbf{M}_1 + \mathbf{M}_2| = |\mathbf{m}|.$$

The weak antiferromagnetism caused by the DM interaction was observed, for example, in the commensurate magnetic phase of the MnSi crystal [6] and one of the antiferromagnetic sublattices of copper ions in the $Ba_3Cu_2O_4Cl_2$ compound [7].

Another cause for canting of the sublattice magnetic moments is noncollinearity of the single-ion anisotropy (SIA) local axes in magnets with several magnetic ions in the crystal unit cell. The single-ion noncollinearity in an antiferromagnet was first examined by Moriya in describing the weak ferromagnetism in a NiF_2 antiferromagnetic crystal with a rutile structure [8] (see also a brief summary of this analysis in book [9]). In this magnet, the easy SIA axes lying in the crystal *ab* planes are mutually orthogonal. The conditions for the occurrence of the SIA-induced noncollinearity were investigated in a symmetric analysis of orthorhombic perovskites [10]. Noncollinearity of the local SIA axes determines, to a great extent, the magnetic properties of ferrites [11]. When the easy axes of sublattices are rotated relative to the common easy axis of a crystal, the collinear ordering becomes unstable against the deviations of moments from the general easy direction due to the occurrence of the linear-in-angle term in the anisotropy energy expansion

$$\epsilon_{a,i} \propto K_i \cos^n(\theta_i - \theta_{Ki}).$$

Here, n is the anisotropy order, θ_i is the angle of orientation of the moment i, and θ_{Ki} is the direction of the anisotropy axis of this moment. Under the condition of noncollinearity of the SIA axes of the moments ($\theta_{Ki} \neq \theta_{Kj}$), this instability, as in the case of the DM interaction, is absolute; i.e., the noncollinearity occurs at any K_i value. A fundamental difference of the single-ion noncollinearity from the DM interaction is its anisotropic character. The SIA energy depends on the moment orientation relative to the crystal axes, while the DM interaction energy is isotropic with the simultaneous rotation of the moments in the plane orthogonal to the vector **D**. In the low-symmetry environment of magnetic ions with the spin $S > 1/2$, a weak ferromagnetic moment is formed by both the

single-ion and two-ion (in particular, DM) anisotropy mechanisms. This manifests itself, first of all, in different dependences of the magnetization curves along different crystal axes. In this case, the competing SIA, depending on the orientation of the magnetic field, can either increase the weak moment or decrease it [12–15]. The orientational spin-flop transition between the states with different orientations of moments in an antiferromagnet can become a first-order phase transition [16]. The conclusion about the dominant effect of the SIA on the formation of a weak ferromagnetic moment was made also for the K_2NiF_4, La_2NiO_4, La_2CoO_4 [13], and $LaMnO_3$ compounds [17, 18].

At present, there is a lack of information on noncollinearity of the magnetic moments caused by the competition of the SIA of crystallographically equivalent sublattices in nonmetal ferromagnets. In magnetic measurements, a weak antiferromagnetic moment is difficult to detect against the background of a strong general magnetization. Such a moment should manifest itself upon reorientation in a magnetic field applied along the weak antiferromagnetism vector (the spin-flop transition). In this case, the longitudinal magnetization abruptly changes. The highly anisotropic character of the magnetization curves of the $PbMnBO_4$ ferromagnetic crystal [19] with a jump of the magnetic moment in the field applied along the orthorhombic *b* axis suggests that the single-ion noncollinearity dominates in this magnet.

The aim of this study is to theoretically describe the orientational phase transition in the framework of a simple model of a ferromagnet with the noncollinear anisotropy axes of two sublattices and determine the dependence of the observed magnetic parameters on the parameters of the local anisotropy of the sublattices.

2. MODEL AND SOLUTIONS

We consider the ground state of a single-position magnet with crystal symmetry plane **m** (or twofold rotation axis C_2) between the translationally nonequivalent positions of magnetic ions. These conditions are typical of magnetic crystals of some groups of the majority class of rhombic crystals, e.g., $PbMnBO_4$ [19–21]. The Hamiltonian of a system of spins with biaxial SIA local axes $z1$, $x1$ and $z2$, $x2$ of two magnetic sublattices can be written in the form

$$H = J\sum_{ij}\mathbf{S}_i\mathbf{S}_j + K_1\left(\sum_i S_i^{z1^2} + \sum_j S_j^{z2^2}\right) + K_2\left(\sum_i S_i^{x1^2} + \sum_j S_j^{x2^2}\right) + g\mu_B\mathbf{H}_0\left(\sum_i \mathbf{S}_i + \sum_j \mathbf{S}_j\right). \quad (1)$$

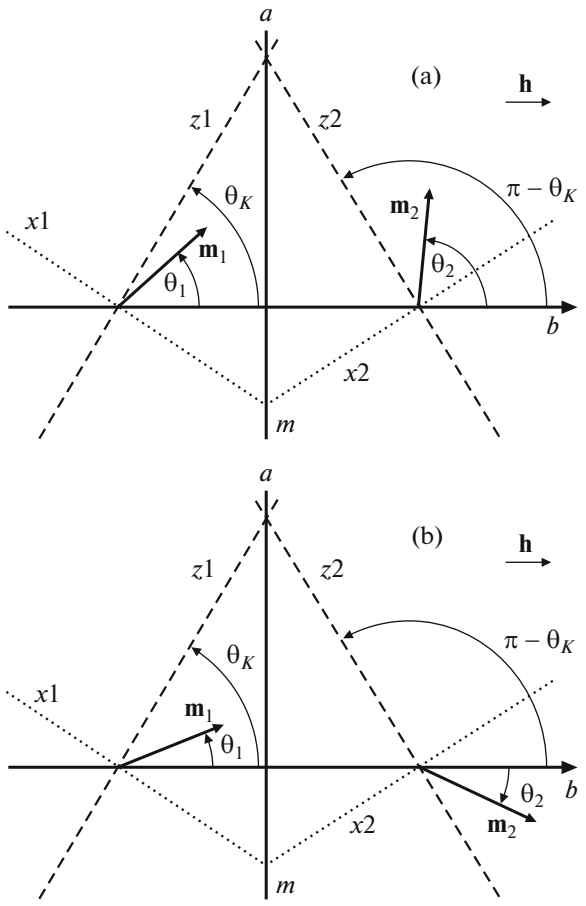

Fig. 1. Orientation of moments m_1 and m_2 of the ferromagnetic sublattices in two different states. At an angle of $\theta_K > \pi/4$ between the easy axes of the sublattices, the ground state is state A at $h < h_{sf}$ and state B at $h > h_{sf}$.

We choose the z_1 and z_2 axes to be easy magnetization axes in each sublattice ($K_1 < 0$). The second local anisotropy constant K_2 (the x_1 and x_2) can have any sign. It can be easily shown that, at the isotropic ferromagnetic exchange ($J < 0$), the moments always lie in the plane formed by the easy axis and external magnetic field directions. For an external magnetic field applied in the plane orthogonal to the symmetry plane **m** and containing the local anisotropy axes K_1 and K_2 of the sublattice moments *i* and *j*, we have a coplanar problem (Fig. 1). This essentially simplifies its solution, which is reduced to finding two sublattice moment orientation angles θ_1 and θ_2 to the external magnetic field direction.

The orthogonality of the local anisotropy axes in each sublattice and the symmetry constraints

$$\theta_{x1} = \theta_{z1} + \pi/2, \quad \theta_{z2} = \pi - \theta_{z1}, \quad \theta_{x2} = \pi - \theta_{x1}$$

allow us to express the anisotropy energy through one effective anisotropy parameter $K = K_1 - K_2$ and the easy axis angle $\theta_K = \theta_{z1}$. In the introduced variables

and designations (Fig. 1), the energy of the ground state of the classical moments $\mathbf{m}_{1,2} = -g\mu_B\mathbf{S}_{1,2}$ has the form

$$E = \frac{N}{2}|J|S^2 z\epsilon(\theta_1, \theta_2),$$

where z is the number of magnetic neighbors,

$$\epsilon(\theta_1, \theta_2) = -\cos(\theta_1 - \theta_2) + a(\cos^2(\theta_1 - \theta_K) + \cos^2(\theta_2 + \theta_K)) - h(\cos\theta_1 + \cos\theta_2),$$

$$a = \frac{K}{|J|z} < 0, \quad \text{and} \quad h = \frac{g\mu_B H_0}{|J|Sz} > 0$$

are the normalized energy, the local anisotropy value, and the external magnetic field, respectively. Minimization of the normalized energy $\epsilon(\theta_1, \theta_2)$ yields the system of two equations

$$\begin{gathered}\sin(\theta_1 - \theta_2) + h\sin\theta_1 \\ - 2a\cos(\theta_1 - \theta_K)\sin(\theta_1 - \theta_K) = 0, \\ -\sin(\theta_1 - \theta_2) + h\sin\theta_2 \\ - 2a\cos(\theta_2 + \theta_K)\sin(\theta_2 + \theta_K) = 0,\end{gathered} \tag{2}$$

which can be transformed to the system of equation for the sum and difference of the moment orientation angles

$$\begin{gathered}h\sin\frac{\theta_1 + \theta_2}{2}\cos\frac{\theta_1 - \theta_2}{2} \\ - a\sin(\theta_1 + \theta_2)\cos(\theta_1 - \theta_2 - 2\theta_K) = 0, \\ \sin(\theta_1 - \theta_2) + h\sin\frac{\theta_1 - \theta_2}{2}\cos\frac{\theta_1 + \theta_2}{2} \\ - a\cos(\theta_1 + \theta_2)\sin(\theta_1 - \theta_2 - 2\theta_K) = 0.\end{gathered} \tag{3}$$

The solutions of Eq. (3) determine two possible states: magnetic phases A and B (Fig. 1)

$$\begin{gathered}\text{A:} \quad \cos\frac{\theta_1 + \theta_2}{2} = \frac{h\cos((\theta_1 - \theta_2)/2)}{2a\cos(\theta_1 - \theta_2 - 2\theta_K)}, \\ \text{B:} \quad \theta_1 = -\theta_2.\end{gathered} \tag{4}$$

The first solution describes the nonsymmetric orientation of the moments of sublattices relative to the magnetic field (the b axis) and the second solution, the symmetric orientation. In zero external magnetic field, the variables and energy states are determined by the equalities

$$h = 0$$

$$\text{A:} \quad \tan\delta_0 = -\frac{a\sin 2\theta_K}{1 + a\cos 2\theta_K}, \quad \delta_0 = \theta_2 - \theta_1|_{h=0},$$

$$\epsilon_{A0} = -\sqrt{1 + a^2 + 2a\cos 2\theta_K};$$

$$\text{B:} \quad \tan 2\theta_0 = -\frac{a\sin 2\theta_K}{1 - a\cos 2\theta_K}, \quad \theta_0 = \theta_{h=0},$$

$$\epsilon_{B0} = -\sqrt{1 + a^2 - 2a\cos 2\theta_K}.$$

Hence, under the conditions

$$a\cos 2\theta_K > 0, \quad \Rightarrow a < 0, \quad \theta_K > \pi/4, \tag{5}$$

$\epsilon_{A0} < \epsilon_{B0}$, the lowest-energy state is phase A with the average magnetization oriented along the a axis (Fig. 1). At $\theta_K < \pi/4$, the b axis turns to the general easy direction and, starting with zero field, phase B is implemented.

Let us consider the change in the orientation of magnetic moments when condition (5) is satisfied in a magnetic field applied along the hard b axis. With an increase in the magnetic field, the angle θ_2 changes faster than the angle θ_1 and, in the field $h = \sqrt{2}a\cos 2\theta_K$, the moments arrange collinearly ($\theta_1 = \theta_2 = \pi/4$). With a further increase in the field, the sign of $\delta = \theta_2 - \theta_1$ can change. However, even earlier, the phase energies can become equal. At this field value $h_{sf} = h(\epsilon_A - \epsilon_B)$, the ground state will change: a phase transition will occur in the magnetic field. Depending on the local anisotropy value a and the easy axes orientation angle θ_K, the transition between phases A and B can be both first- and second-order. The ground state evolution in an external field at $a = -0.1$ and $\theta_K = 0.9$ is illustrated in Fig. 2. The investigated orientational phase transition is obviously analogous to the spin-flop transition in a conventional antiferromagnet. At $h \to 0$, the field is directed along the weak antiferromagnetism vector $\mathbf{l} = \mathbf{m}_1 - \mathbf{m}_2$. After the transition, the vector $\mathbf{l}$ is oriented orthogonally to the external field (Fig. 1).

Since the discussed model can have different solutions, it is important to determine a stability region for each state. In the case of the first-order phase transition, this provides information on the possible magnetization hysteresis value. The stability regions for solutions (4) are determined by the positive determinacy of the main minors of the determinant [22]

$$\left\|\partial^2\epsilon/\partial\theta_n\partial\theta_m\right\|, \quad (n, m = 1, 2).$$

At $|a|, h \ll 1$, we have $\partial^2\epsilon/\partial\theta_{1,2}^2 > 0$ and the equation

$$\frac{\partial^2\epsilon}{\partial\theta_1^2}\frac{\partial^2\epsilon}{\partial\theta_2^2} - \frac{\partial^2\epsilon}{\partial\theta_1\partial\theta_2}\frac{\partial^2\epsilon}{\partial\theta_2\partial\theta_1} = 0$$

together with energy minimization equations (2) for each phase (4) determines the phase stability boundaries h_{as} and h_{bs}. The overlap of the stability regions determines the field range of the possible magnetization hysteresis. This range depends, to a great extent, on the anisotropy axis orientation angle θ_K and, at $a = -0.1$, turns to zero at $\theta_K \approx 1.01$ (Fig. 3). The boundaries coincide with the transition field h_{sf}, which corresponds to a second-order phase transition. A change in the phase transition type is discussed in Section 4. When the angle of rotation of the anisotropy axes is close to $\pi/4$ ($\theta_K < \theta_{K0} = 0.5\arccos a$), phase B is

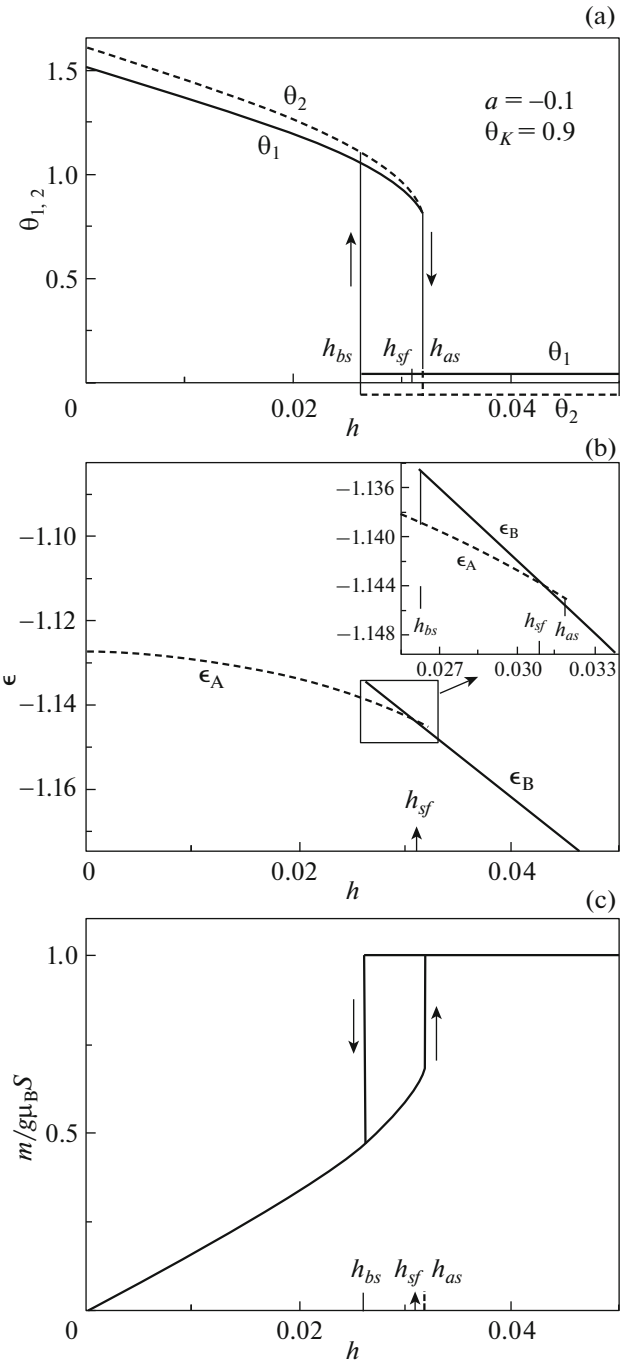

Fig. 2. Field dependences of (a) the angles θ_1 and θ_2 of orientation of the sublattice magnetic moments, (b) the energies of phases A and B, and (c) the magnetization projection onto the external field direction at a relative local anisotropy of $a = -0.1$ and an easy anisotropy axis orientation angle of $\theta_K = 0.9$. Inset in (b): enlarged region of intersection of the phase energies ϵ_A and ϵ_B. Vertical arrows show the direction of the change in the angles $\theta_{1,2}$, energy, and longitudinal magnetization at the boundaries h_{as} and h_{bs} of stability of phases A and B, respectively. h_{sf} is the field at which the phase energies coincide.

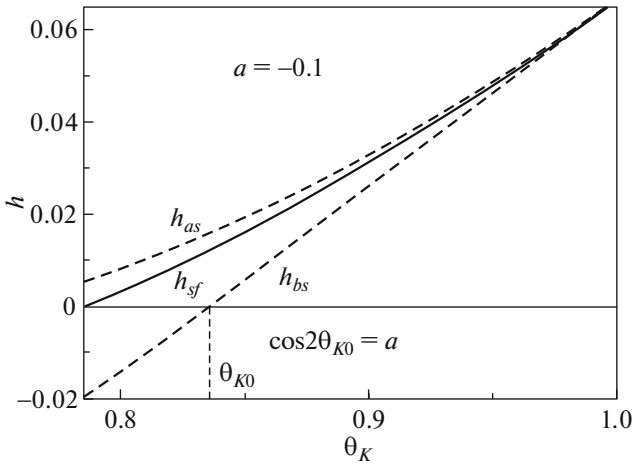

Fig. 3. Dependence of the boundaries of stability of phases A (h_{as}) and B (h_{bs}) (dashed lines) on the anisotropy axis orientation angle θ_K at an anisotropy parameter of $a = -0.1$.

stable in any magnetic field (the stability boundary is $h_{bs} < 0$).

3. SUSCEPTIBILITY

Each type of magnetic ordering is characterized by the dependence of the magnetic moment on the applied field value and direction. As a rule, the magnetization projection onto the applied field direction, i.e., the longitudinal magnetization, is measured. Although in the case of a complex, e.g., noncollinear magnetic structure, this information is insufficient, it reflects the integral anisotropic properties of a magnet. The initial portion in the field dependence of the longitudinal magnetization in the field applied along the hard direction of a magnetic crystal brings information about the magnetic anisotropy value, which, in the case of a collinear ferromagnet, makes it possible to determine this value even in relatively weak fields. However, if the local axes of sublattices are noncollinear, we deal with some effective anisotropy averaged over its local values. This yields the general anisotropy of the entire magnet, which is lower than the local values [11]. Consequently, the slope of the magnetization curves (the initial susceptibility) can significantly increase at the large noncollinearity $\theta_K \to \pi/4$ as compared with the case of a collinear ferromagnet with $\theta_K = \pi/2$ ($\chi(\theta_K = \pi/2)$) (Fig. 4).

4. PHASE DIAGRAM

The dependence of the spin-flop transition field on the angle of rotation of the anisotropy axes determines the boundary between low-field phase A and high-field phase B, i.e., the angle–field phase diagram (Fig. 5). The asymptotic values of the field h_c of com-

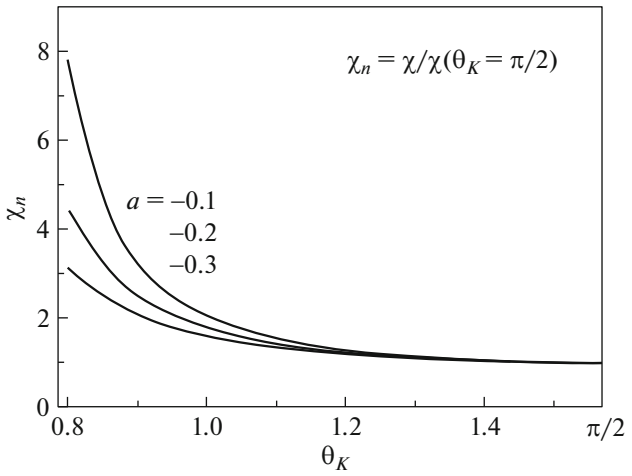

Fig. 4. Dependence of the initial susceptibility normalized to the susceptibility of a collinear ferromagnet ($\chi(\theta_K = \pi/2)$) on the anisotropy axis orientation angle θ_K at different anisotropy parameters a.

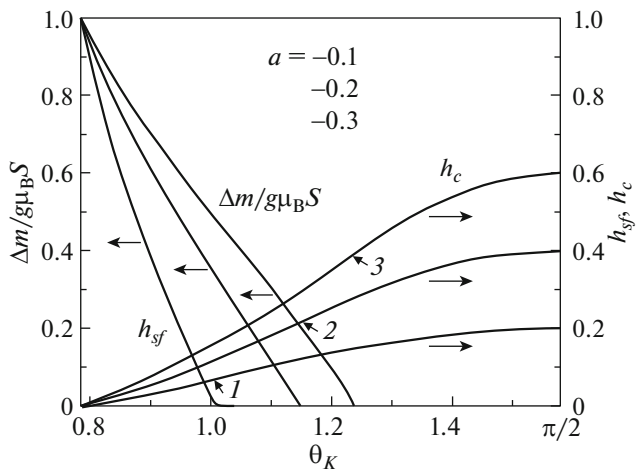

Fig. 5. Dependence of the spin-flop transition field h_{sf} (the interfaces) and the jump of the relative longitudinal magnetization $\Delta m_1/g\mu_B S$ on the anisotropy axis orientation angle θ_K at anisotropy parameters of $a = -0.1$, -0.2, and -0.3. Numerals *1*, *2*, and *3* indicate the critical fields above which the phase transition becomes second-order ($h_{sf} \to h_c$) at local anisotropy parameters of $a = -0.1$, -0.2, and -0.3, respectively.

pletion of the reorientation by the second-order phase transition at $\theta_K \to \pi/2$ correspond to the case of a collinear ferromagnet:

$$h_c\left(\theta_K = \frac{\pi}{2}\right) = -2a.$$

At $\theta_K \to \pi/4$, the general anisotropy disappears and the noncollinear moments rotate toward the magnetization direction in an arbitrarily weak field. The same happens in the other limiting case of the uniaxial easy-plane anisotropy $a = 0$ ($K_1 = K_2$ (1)).

The same diagram shows the dependence of the jump in the relative magnetization during the spin-flop transition on the anisotropy axis orientation angle. With an increase in the angle (upon approaching the collinear case), this jump rapidly decreases and, at points *1*, *2*, and *3* in the transition field curves at $a = -0.1$, -0.2, and -0.3, respectively, turns to zero. Above these values, the orientational transition is completed with a second-order phase transition with the critical field h_c.

The type of the phase transition between states (4) is determined by the anisotropy parameters. The longitudinal magnetization jump occurring upon completion of the orientational transition from phase A to phase B is threshold in the anisotropy parameters a and θ_K. The relation between these parameters at which the jump occurs (i.e., the transition becomes first-order) can be obtained from the limiting condition for the existence of phase A

$$\theta_1 = -\theta_2 = \theta_c$$

at the point of crossing of the phase energies ϵ_A and ϵ_B (Fig. 2b). In this case, the θ_c value coincides with the angle θ of phase B. The curves in Fig. 2b at the limit applied field h_c touch one another

$$\frac{d\epsilon_A}{dh} = \frac{d\epsilon_B}{dh}.$$

Above this value, system (2) has no solution for phase A. At the small noncollinearity of the sublattices $\theta_2 - \theta_1 \ll 1$ (weak antiferromagnetism), the imposed conditions lead to the values

$$\sin 2\theta_c \approx -a \sin 2\theta_K, \quad h_c \approx 2a \cos 2\theta_K. \qquad (6)$$

The general numerical solution of the conditions distinguishes the regions with different phase transition types on the plane of the anisotropy parameters (Fig. 6).

A necessary condition for the completion of the sublattice reorientation in a magnetic field with the first-order transition is the SIA-induced noncollinearity of the magnetic moments. It leads to the occurrence of two minima in the angular dependence of the total anisotropy energy and, as a result, to two minima in the field dependence of the energy of the ground state (phases A and B). A more rapid change in the minimum of phase A leads to the coincidence of the minima of the phases until their merging. In this case, the intersection of the phase energies occurs before the reorientation of the moments of phase A (Fig. 2b); i.e., the orientational transition ends with a first-order phase transition.

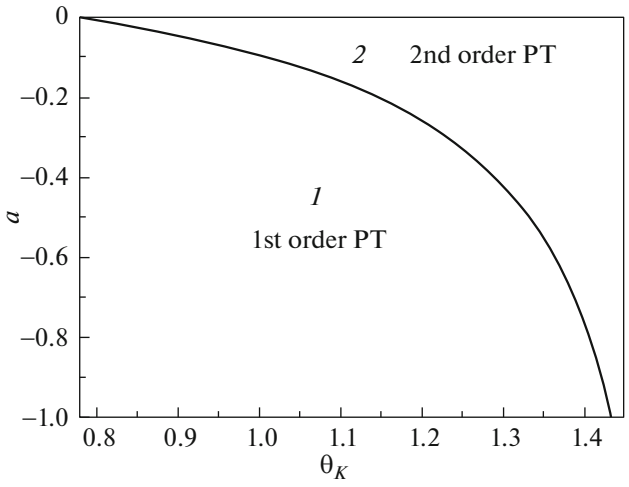

Fig. 6. Two regions on the plane of the anisotropy parameters with the different types of the orientational phase transition. In region *1* (the first-order phase transition (PT)), the reorientation ends with a first-order phase transition and, in region *2* (the second-order order PT), with a second-order transition.

5. DISCUSSION

In the investigated model, two SIA parameters, a and θ_K, determine four values that can be found from the experimental magnetization curve, specifically, the curve slope (the initial susceptibility) (Fig. 4), the transition field, the magnetization jump value (Fig. 5), and the magnetic field hysteresis width (Fig. 3). The last two quantities are most difficult to determine. Taking into account the increasing steepness of the curve upon approaching the field h_{sf}, the need for the accurate crystal orientation relative to the external field, and the strong temperature dependence of the magnetization curve [19], it is difficult to accurately determine the magnetization jump value. The hysteresis width can significantly depend on the speed of passing the transition point. The simplest seems to be the determination of the SIA parameters from the first two experimental values, i.e., the initial susceptibility and the transition field.

The magnetic anisotropy of $PbMnBO_4$ is determined by the strong Jahn–Teller distortion of the oxygen octahedra surrounding Mn^{3+} copper ions [19]. In this case, the long axis is considered to be a local easy SIA axis. Distorted octahedra form chains along the b axis with the strongest ferromagnetic exchange between manganese ions. The planes containing the long and short axes of the octahedra are rotated relative to the common easy orthorhombic crystal a axis by an angle of $\phi \approx 30°$ (the projection of the orthorhombic axis a is shown in Fig. 1). Thus, the energy of the resulting SIA depends on the orientation of the moments of four exchange-coupled translationally nonequivalent sublattices and, therefore, is determined by both the local anisotropy and the values of exchange interactions within and between the chains. The effective constant is not a simple sum of the local ones multiplied by the function of the angles θ_{Ki} nor is the effective SIA a simple sum of any local projections. The comparison of the calculated magnetization curves with the experimental dependence observed for $PbMnBO_4$ in a field applied along the orthorhombic b axis [19] yields the anisotropy parameters $a \approx -0.1$ and $\theta_K \approx 0.9$. The obtained angle of orientation of the local easy axis is similar to the angle of orientation of the long diagonal of the distorted oxygen octahedron surrounding Mn^{3+} ions relative to the b axis ($\theta = 0.84$). To make a comparison with the SIA value along the orthorhombic a axis (the effective macroscopic anisotropy) determined within the single-sublattice model [23], we use the exchange interaction value J obtained in this study. The value $a \approx -0.1$ obtained here using two-sublattice model (1) exceeds the effective anisotropy by a factor of almost 3 [23]. Noncollinearity of the local anisotropy axes in a multi-sublattice ferromagnet (or an antiferromagnet [16]) yields not only the characteristic nonlinear magnetization curve with a magnetic moment jump, but also always a smaller value of the observed macroscopic anisotropy as compared with the local value by effective averaging of the anisotropy of noncollinear sublattices [11]. A detailed analysis of the anisotropic properties of $PbMnBO_4$, including the magnetization along the hardest c axis, using the four-sublattice model with regard to the orientation of the axes of octahedra and the effect of the DM interaction requires special investigations and will be presented elsewhere. We only note that the combined influence of the SIA and the DM interaction in this magnet preserves the general form of the magnetization curve and the spin-flop transition in a field applied along the orthorhombic b axis.

At present, the increasing interest in noncollinear magnets is mainly due to the magnetoelectric properties that accompany magnetic noncollinearity [24, 25]. This interest is dictated, first of all, by the possibility of controlling the magnetic parameters of a crystal by changing the electric polarization and vice versa, which has a great potential for technology. An ideal magnetoelectric multiferroic should be a crystal in which a high spontaneous polarization would be related to a strong magnetization [15]. Then, the most striking manifestation of the magnetoelectric properties should be expected at an abrupt change in the orientation of such magnetization in the vicinity of a first-order phase transition. At such a transition, the magnetization jump in a weak antiferromagnet can be much greater than the analogous jump in a weak ferromagnet. In addition, an important advantage is a much weaker field of the spin-flop transition in a weak antiferromagnet, which is only determined by the SIA. Note that, in the isostructural $PbFeBO_4$ crystal,

anomalies of the dielectric properties were detected at the temperature of establishing of the short- and long-range magnetic order, which points out the correlation between the magnetic and electric subsystems in this crystal [26].

6. CONCLUSIONS

In a ferromagnet with the noncollinear single-ion anisotropy axes of the magnetic sublattices, the orientational phase transition in a field applied in the plane containing the local anisotropy axes can occur either in the form of two second-order phase transitions with a continuous rotation of the sublattice moments or in the form of one second-order transition and one first-order transition. In the latter case, the first-order (spin-flop) transition is accompanied by a jump in the magnetization projection onto the applied field direction and by the hysteresis. The transition is threshold in the anisotropy parameters, i.e., the value of the local anisotropy and orientation of its axes, and occurs in a wide range of these parameters. The dependences of the spin-flop transition field, magnetization jump, initial susceptibility, and boundary of the occurrence of the first-order phase transition on the sublattice local anisotropy parameters were obtained. The comparison with the experimental magnetization curves for the $PbMnBO_4$ compound made it possible to numerically estimate the local anisotropy parameters for the two-sublattice model and conclude that the anisotropy is effectively averaged upon rotation of the axes.

ACKNOWLEDGMENTS

The author thanks A.I. Pankrats and A.D. Balaev for useful discussion.

FUNDING

This study was supported by the Russian Foundation for Basic Research, the Government of the Krasnoyarsk krai, and the Krasnoyarsk Territorial Foundation for Support of Scientific and R&D Activity, project no. 18-42-240008 "Effect of the Magnetic Structure on the Magnetodielectric Properties of Oxide Crystallites Containing Stereoactive Pb^{2+} and Bi^{3+} Ions."

CONFLICT OF INTEREST

The authors declare that they have no conflicts of interest.

REFERENCES

1. S. V. Vonsovsky and A. A. Turov, J. Appl. Phys. **30**, 9S (1959).
2. S. V. Vonsovskii, *Magnetism* (Nauka, Moscow, 1971), p. 754.
3. E. A. Turov, *Physical Properties Of Magnetically Ordered Crystals* (Akad. Nauk SSSR, Moscow, 1963), p. 177 [in Russian].
4. I. Dzyaloshinsky, J. Phys. Chem. Solids **4**, 241 (1958).
5. T. Moriya, Phys. Rev. **120**, 91 (1960).
6. V. E. Dmitrienko and V. A. Chizhikov, Phys. Rev. Lett. **108**, 187201 (2012).
7. V. Yushankhai, M. Wolf, K.-H. Muller, R. Hayn, and H. Rosner, Phys. Rev. B **62**, 14229 (2000).
8. T. Moriya, Phys. Rev. **117**, 635 (1960).
9. J. S. Smart, *Effective Field Theories of Magnetism* (Saunders, London, 1966; Mir, Moscow, 1968), p. 177.
10. E. F. Bertaut, in *Magnetism, Collection of Articles* (Academic, New York, 1963), Vol. 3, p. 149.
11. S. Krupička, *Physics of Ferrites and Related Magnetic Oxides* (Prague, Academy, 1973), Vol. 2.
12. E. A. Turov, A. V. Kolchanov, V. V. Men'shenin, I. F. Mirsaev, and V. V. Nikolaev, *Symmetry and Physical Properties of Antiferromagnetics* (Fizmatlit, Moscow, 2001), p. 103 [in Russian].
13. D. Coffey, J. Appl. Phys. **70**, 6326 (1991).
14. G. A. Petrakovskii, M. A. Popov, A. D. Balaev, K. A. Sablina, O. A. Bayukov, D. A. Velikanov, A. M. Vorotynov, A. F. Bovina, A. D. Vasil'ev, and M. Boehm, Phys. Solid State **51**, 1853 (2009).
15. C. Weingart, N. Spaldin, and E. Bousquet, Phys. Rev. B **86**, 094413 (2012).
16. S. N. Martynov, JETP Lett. **108**, 196 (2018).
17. D. Talbayev, L. Mihaly, and J. Zhou, Phys. Rev. Lett. **93**, 017202 (2004).
18. A. A. Mozhegorov, L. E. Gonchar, and A. E. Nikiforov, Low Temp. Phys. **33**, 229 (2007).
19. A. Pankrats, K. Sablina, M. Eremin, A. Balaev, M. Kolkov, V. Tugarinov, and A. Bovina, J. Magn. Magn. Mater **414**, 82 (2016).
20. H. Park and J. Barbier, Acta Crystallog. E **57**, 82 (2001).
21. H. Park, R. Lam, J. E. Greedan, and J. Barbier, Chem. Matter. **15**, 1703 (2003).
22. Yu. A. Izyumov and V. R. Syromyatnikov, *Phase Transitions and Crystal Symmetry* (Nauka, Moscow, 1984), p. 105 [in Russian].
23. A. Pankrats, M. Kolkov, S. Martynov, S. Popkov, A. Krasikov, A. Balaev, and M. Gorev, J. Magn. Magn. Mater **471**, 416 (2019).
24. T. Kimura, T. Goto, H. Shintani, K. Ishizaka, T. Arima, and Y. Tokura, Nature (London, U. K.) **426**, 55 (2003).
25. E. Bousquet and A. Cano, J. Phys.: Condens. Matter **28**, 1 (2016).
26. A. Pankrats, K. Sablina, D. Velikanov, A. Vorotynov, O. Bayukov, A. Eremin, M. Molokeev, S. Popkov, and A. Krasikov, J. Magn. Magn. Mater. **353**, 23 (2014).

Translated by E. Bondareva